Antiviral Research 169 (2019) 104544

Contents lists available at ScienceDirect

Antiviral Research

journal homepage: www.elsevier.com/locate/antiviral

A HTRF based competitive binding assay for screening specific inhibitors of HIV-1 capsid assembly targeting the C-Terminal domain of capsid

Da-Wei Zhang[a,c,1], Rong-Hua Luo[b,1], Lei Xu[a,1], Liu-Meng Yang[b], Xiao-Shuang Xu[a], Gregory J. Bedwell[c], Alan N. Engelman[c], Yong-Tang Zheng[b,**], Shan Chang[a,*]

[a] Institute of Bioinformatics and Medical Engineering, School of Electrical and Information Engineering, Jiangsu University of Technology, Changzhou, 213001, China
[b] Key Laboratory of Animal Models and Human Disease Mechanisms of the Chinese Academy of Sciences, KIZ-CUHK Joint Laboratory of Bioresources and Molecular Research in Common Diseases, The National Kunming High Level Biosafety Research Center for Nonhuman Primate, Kunming Institute of Zoology, Chinese Academy of Sciences, Kunming, Yunnan, 650223, China
[c] Department of Cancer Immunology and Virology, Dana-Farber Cancer Institute and Department of Medicine, Harvard Medical School, 450 Brookline Avenue, Boston, MA, 02215, USA

ARTICLE INFO

Keywords:
HIV-1 capsid
Capsid C-Terminal domain
Drug discovery
TX-1918
HTRF

ABSTRACT

Due to its multifaceted essential roles in virus replication and extreme genetic fragility, the human immunodeficiency virus type 1 (HIV-1) capsid (CA) protein is a valued therapeutic target. However, CA is as yet unexploited clinically, as there are no antiviral agents that target it currently on the market. To facilitate the identification of potential HIV-1 CA inhibitors, we established a homogeneous time-resolved fluorescence (HTRF) assay to screen for small molecules that target a biologically active and specific binding pocket in the C-terminal domain of HIV-1 CA (CA CTD). The assay, which is based on competition of small molecules for the binding of a known CA inhibitor (CAI) to the CA CTD, exhibited a signal-to-background ratio (S/B) > 10 and a Z' value > 0.9. In a pilot screen of three kinase inhibitor libraries containing 464 compounds, we identified one compound, TX-1918, as a low micromolecular inhibitor of the HIV-1 CA CTD-CAI interaction (IC_{50} = 3.81 μM) that also inhibited viral replication at moderate micromolar concentration (EC_{50} = 15.16 μM) and inhibited CA assembly *in vitro*. Based on the structure of TX-1918, an additional compound with an antiviral EC_{50} of 6.57 μM and cellular cytotoxicity CC_{50} of 102.55 μM was obtained from a compound similarity search. Thus, the HTRF-based assay has properties that are suitable for screening large compound libraries to identify novel anti-HIV-1 inhibitors targeting the CA CTD.

1. Introduction

Human immunodeficiency virus type 1 (HIV-1) infects and kills $CD4^+$ T cells in patients, who normally exhibit CD4 decline and immunodeficiency, eventually resulting in acquired immunodeficiency syndrome (AIDS) (Hel et al., 2006). Over the past decades, approximately 30 drugs have been approved for use against HIV infection, targeting several critical steps in the virus replication cycle (Chaudhuri et al., 2018). These drugs coupled with the introduction of antiviral combination therapy has led to a dramatic decrease of mortality and prolonged life expectancy of HIV positive patients. As a result, HIV-1 infection can be managed effectively as a chronic disease (Engelman and Cherepanov, 2012). However, the treatment is not a cure, and treatment success can be compromised by the unwanted side effects of current medications and by the emergence of drug-resistant viral strains (Zhang, 2018). Consequently, there continues to be a need for new drugs with superior characteristics (e.g., reduced toxicity and more convenient dosing regimens) and novel mechanisms of action.

The HIV-1 capsid (CA) represents an attractive yet clinically unexploited target. Approved antiretroviral drugs target four viral proteins (reverse transcriptase, protease, integrase and gp41) and one host protein (CCR5) (https://www.fda.gov/ForPatients/Illness/HIVAIDS/Treatment/u.

cm118915.htm). None of these FDA-approved drugs directly inhibits CA, which notably participates in numerous steps of the HIV-1 replication cycle including virus assembly, maturation, uncoating, nuclear import, reverse transcription and integration (Campbell and Hope, 2015). Retroviruses such as HIV-1 replicate via RNA intermediates and

* Corresponding author.
** Corresponding author.
E-mail addresses: zhengyt@mail.kiz.ac.cn (Y.-T. Zheng), schang@jsut.edu.cn (S. Chang).
[1] These authors contributed equally to this work.

https://doi.org/10.1016/j.antiviral.2019.104544
Received 1 October 2018; Received in revised form 13 June 2019; Accepted 20 June 2019
Available online 27 June 2019
0166-3542/

Table 1
Capsid-targeting compounds.

Compound	Binding site on CA	EC_{50} (μM)	Type	Clinical trials	Reference
CAP-1	CA NTD	≈70	Small molecule	No	Tang et al. (2003)
CAI	CA CTD	Not done	peptide	No	Sticht et al. (2005)
NYAD-1	CA CTD	4–22	stapled peptide	No	Zhang et al. (2008)
NYAD201	CA CTD	1.58-9.88	stapled peptide	No	Zhang et al. (2011)
BD-1	CA NTD	0.07	Small molecule	No	Lemke et al. (2012)
BM-1	CA NTD	0.06	Small molecule	No	Lemke et al. (2012)
PF-3450074 (PF74)	CA NTD	0.3–0.6	Small molecule	No	Blair et al. (2010); Shi et al. (2011)
BMMP	Unknown	20–50	Small molecule	No	Urano et al. (2011)
BI-1	CA NTD	1.4	Small molecule	No	Lamorte et al. (2013); Price et al. (2014)
BI-2	CA NTD	1.8	Small molecule	No	Lamorte et al. (2013); Price et al. (2014)
Ebselen	CA CTD	3.37	Small molecule	No	Thenin-Houssier et al. (2016)
GS-CA1	CA NTD	0.00014	Small molecule	Yes	Tse et al. (2017)
Compound 1	CA NTD	57	Small molecule	No	Lemke et al. (2013)
Coumermycin A1	CA NTD	8	Small molecule	No	Chen et al. (2016); Vozzolo et al. (2010)
I-XW-053	CA NTD	22.5	Small molecule	No	Kortagere et al. (2012), 2014
Compound 27	CA CTD	4.6	Small molecule	No	Machara et al. (2016)
Compound 40	CA CTD	35	Small molecule	No	Kožíšek et al. (2016)
NYAD-36	CA-CTD	1.5	stapled peptide	No	Zhang et al. (2013)
Compound 50	CA-CTD	1.1–10.9	Small molecule	No	Curreli et al. (2011)
Compound 6	CA-CTD	1.6–6.2	Small molecule	No	Curreli et al. (2011)
GDC	CA-CTD	3.12	Small molecule	No	Lampel et al. (2015)
TA	CA-CTD	~50% at 100 μM	Small molecule	No	Lampel et al. (2015)
κFGF-MTS-anti-p24-mAb	Unknown	~73% at 10 μg/ml	Antibody	No	Ali et al. (2016)

accordingly exhibit comparatively high mutation rates. Genetic robustness (i.e., the ability to tolerate mutations) underlies preservation of function in the face of sequence change (Elena, 2012) and could be leveraged to design novel antiretroviral compounds. HIV-1 CA notably exhibits extreme genetic fragility, suggesting that CA is a good target for therapy and vaccination strategies (Rihn et al., 2013).

HIV-1 CA protein originates from the 55-kDa Gag polyprotein precursor and is composed of two independently folded domains, the N-terminal domain (CA- NTD; residue 1–145) and C-terminal domain (CA-CTD, residues 151–231), which are connected by a 5-residue flexible linker (Tedbury and Freed, 2015). Despite its attractiveness as a drug target, less than two dozen CA-targeting compounds, which include small molecules, peptides and an antibody, by our count have been described (summarized in Table 1). So far, none of these candidates has been licensed for clinical use. Fortunately, the promising compound GS-CA1, which blocks both disassembly and assembly and yields defective virions, has been evaluated in a phase 1 clinical trial (Perrier et al., 2017; Tse et al., 2017; Carnes et al., 2018). Of the 10 compounds previously described to target the CA CTD, the 12-residue CAI peptide ITFEDLLDYYG (for capsid assembly inhibitor) efficiently abrogated the assembly of both immature and mature CA structures *in vitro*. NMR, X-ray crystallography and mutation analyses revealed that CAI binds specifically to a reactive hydrophobic pocket in the CA CTD (Sticht et al., 2005; Ternois et al., 2005). Due to its lack of cell permeability, CAI antiviral activity could not be assessed in cell culture. However, its cell-penetrating derivative, the stapled peptide NYAD-1, could inhibit HIV-1, validating the CAI-binding pocket as a target for HIV-1 CA assembly inhibitors (Zhang et al., 2008).

Here, based on homogeneous time-resolved fluorescence (HTRF) technology, we developed a novel assay for screening small compounds targeting the same pocket as CAI to identify lead antiviral compounds. Three libraries composed of 464 protein kinase inhibitors in total were screened to validate the use of HTRF for the identification of inhibitors of HIV-1 CA. This mix-and-read and wash-free assay is scalable to a 384-well format and sufficiently robust for high-throughput screening (HTS).

2. Materials and methods

2.1. Agents and inhibitor libraries

XL665-conjugated streptavidin (Lyophilized) and monoclonal antibody (Mab) anti-GST-Eu cryptate (Lyophilized) were purchased from Cisbio Bioassays (Bedford, MA, USA). Black microplates (96-well) were purchased from Greiner Bio-One (Darmstadt, Germany). White 384-shallow well microplates were purchased from PerkinElmer (Boston, MA). Streptavidin (SA) biosensors were purchased from Pall ForteBio (Fremont, CA, USA). Peptides were custom synthesized by GL Biochem (Shanghai) Ltd. Ebselen and taurocholic acid were purchased from MedChem Express (Shanghai, China). Glycodeoxycholate was purchased from Shanghai Macklin Biochemical Co., Ltd. Working stocks of these chemicals were prepared by dissolution in dimethyl sulfoxide (DMSO) to 10 mM concentrations. Three protein kinase inhibitor libraries (Syn kinase inhibitor library, protein kinase inhibitor library and kinase inhibitor library) were obtained from National Compound Resource Center (Shanghai, China). Ni-nitriloacetic acid (NTA) and glutathione S-transferase (GST) resins were purchased from Smart-Lifesciences (Changzhou, China). The anti-p24 antibody was homemade (Liu et al., 2007) and anti-β-actin antibody was obtained from CWBIO (China). Polyvinylidene fluoride (PVDF) membranes and chemiluminescent horse radish peroxidase (HRP) substrate were purchased from Millipore (USA). Cell lysis buffer for western blotting was purchased from Beyotime (China). All general biochemical reagents were obtained from AMRESCO (Solon, USA). HIV-1 inhibitors tenofovir disoproxil fumarate (TDF) and indinavir (IDV) were obtained from Medical Research Council, AIDS Reagent Projects.

2.2. Cells and virus

Human T cell lines MT-4 and C8166, as well as laboratory-derived virus HIV-1_{IIIB}, were obtained from Medical Research Council, AIDS Reagent Project. Cells were maintained in RPMI medium 1640 (Gibco) containing 10% fetal bovine serum (FBS, Gibco), 100 units/ml penicillin and 100 units/ml streptomycin. HIV-1_{IIIB} was propagated in C8166 cells.

2.3. Expression and purification of recombinant CA CTD and full-length CA proteins

DNA encoding the C-terminal 89 amino acids of CA was codon optimized for expression in *Escherichia coli* and chemically synthesized by Genewiz, Inc. (Suzhou, China). The resulting sequence was subcloned into *Bam*HI-*Not*I sites of a pGEX-4T-1 expression plasmid harboring the N-terminal GST tag. Recombinant CA CTD protein was expressed in *E. coli* BL21(DE3) and purified as previously described (Thenin-Houssier et al., 2016). Expression and purification of full-length wild type CA (CA-WT) in *E. coli* using plasmid pET11a CA-WT was done as previously described (Lanman et al., 2002). Concentrations of proteins were determined by the Bradford assay using bovine serum albumin (BSA) as a standard. Proteins were analyzed using 12% sodium dodecyl sulfate-polyacrylamide gel electrophoresis (SDS-PAGE) to asses purity.

2.4. K_D determination of the interaction between CA CTD and CAI

Biolayer interferometry was measured using an OctetRED96 instrument in combination with streptavidin functionalized biosensors. All assays were run at 30 °C with continuous 1000 rpm shaking. Phosphate-buffered saline (PBS) with 0.01% Tween-20 was used as the assay buffer. Loading of biosensors was conducted by exposing samples containing 10 μg/ml biotin-CAI to pre-equilibrated biosensor tips for 300 s. Association of samples containing increasing amounts GST-CA CTD was recorded for 800 s from drop-holder position. Dissociation was measured by dipping the biosensor tip into a tube filled with assay buffer for 800 s. Reference measurements were conducted by using buffer instead of CA CTD samples, and reference signals were subtracted from experimental samples to obtain final signals. Global 1:1 fitting of association and dissociation curves with Fortebio data analysis 9.0 software revealed k_{on}, k_{dis} and K_D binding constants. GraphPad Prism 5.0 was used to visualize curves.

2.5. HTRF-based CAI binding competition assay

An HTRF assay was used to measure the interaction between the CA CTD and CAI. The experiment was performed in white 384-shallow well microplates in PBS supplemented to contain 0.05% Tween 20 and 2 mM β-mercaptoethanol using the PerkinElmer Enspire plate reader. First, 1 μl reaction buffer, 2 μl CAI-biotin peptide (ITFEDLLDYYGPGGGSK-biotin) and 2 μl GST-CA CTD were added to the plate. After incubation at room temperature for 30 min, 5 μl of premixed fluorescent donor (anti-GST europium cryptate) and fluorescent acceptor (XL665-conjungated streptavidin) in assay buffer with 100 mM potassium fluoride (KF) was added. Following an additional 1 h at room temperature, the plate was read in an Envision multilabel reader. Raw counts per s (cps) were collected at 665 nm and 620 nm, and the signal was calculated as: (cps 665 nm/cps 620 nm) × 10,000. Buffer instead of both proteins was used as negative control. DMSO instead of compound was used as a positive control. Untagged CAI was used as a positive compound for inhibition of GST-CA CTD/CAI. Compounds were dispensed into the assay plate wells prior to the addition of the assay mixture. GraphPad Prism was used to visualize does response curves and to calculate IC_{50} values by plotting inhibition values against logarithmic compound concentrations and applying a sigmoidal dose-response fit (variable slope).

The assay was optimized to achieve a satisfactory signal-to-background ratio (S/B) by adjusting the amounts of CA CTD protein, CAI peptide and DMSO in the assay mixture. S/B is widely used to indicate the quality of an assay. For good quality, the minimum value of S/B should be greater than 3. The competence of the assay in 384-well plates was evaluated by preparing a checkerboard plate, in which the assay mixture with CAI (positive samples) and without CAI (for background binding) were distributed in alternating wells. Data were analyzed in GraphPad Prism 5.0.

2.6. Assay validation for high-throughput screening

Stock solutions of Syn kinase Inhibitor Library (86 compounds), Protein Kinase Inhibitor Library (282 compounds) and Kinase Inhibitor Library (96 compounds) were available at 10 mM concentrations in DMSO. For HTS, the volume of the assay was miniaturized to 10 μl total with a 384-well plate. The protein, the peptide and the test compounds were mixed together and incubated for 30 min at room temperature, then the two fluorophores were added. The mixture was incubated for 1 h at room temperature before the emission was read at 665 nm and 620 nm. The HTRF signal was calculated as a ratio of emission: (665 nm/620 nm) × 10,000. All plates were analyzed and passed quality control (QC) if their Z′-factor was greater than 0.5. Data were analyzed visualized in GraphPad Prism 5.0.

Z′-factor (Zhang et al., 1999) to estimate assay quality was calculated using the following equation:

$$Z' = 1 - \frac{3 \times SDmax + 3 \times SDmin}{|\mu max - \mu min|}$$

where SD_{max} and SD_{min} are standard deviations of the positive and negative control measurements, respectively, and μmax and μmin are the mean of the respective positive and negative signal controls.

2.7. Effects of TX-1918 on in vitro CA assembly

Purified CA-WT protein was dialyzed against 50 mM sodium phosphate, pH 8.0 buffer. *In vitro* assembly assays were performed as previous described (Lanman et al., 2002). Compound was added to CA-WT (final concentration of 50 μM) in 50 mM sodium phosphate buffer, pH 8.0 in a volume of 500 μl. CA assembly was initiated by addition of 500 μl 50 mM sodium phosphate buffer containing 4 M NaCl, pH 8.0. Optical density was monitored on a spectrophotometer at 350 nm every 20 s for 30 min.

2.8. Cytotoxicity assays

The cytotoxicity of the compounds was determined by MTT colorimetric assay described previously (Wang et al., 2004). C8166 or MT-4 cells (4×10^4/well) were co-incubated with serial diluted compounds in 96-well plates at 37 °C in humidified tissue culture incubators containing 5% CO_2. After 3 days, cell viability was determined using MTT, and the 50% cytotoxicity concentration (CC_{50}) was calculated.

2.9. Cytopathic effect assay

Anti-HIV-1 activity was evaluated via inhibition of virus-induced cytopathic effects (Wang et al., 2011). Briefly, C8166 cells (4×10^4/well) were infected with HIV-1_{IIIB} at a multiplicity of infection (M.O.I) of 0.03, with vehicle control or serially diluted compounds in 96-well plates at 37 °C, 5% CO_2. After 3 days, the cytopathic effect was accessed by light microscopy by counting the number of syncytia in each well, and 50% effective concentrations (EC_{50}) were calculated. The selectivity index (SI) was determined as CC_{50} divided by EC_{50}. TDF was used as a positive control.

2.10. Analogues chosen by similarity search

Analogues of compound TX-1918 were chosen from the ChemDiv database by similarity search on the basis of the Tanimoto similarity coefficients evaluated in the MACCS structural fingerprints of Molecular Operating Environment (MOE) suite (Willett, 2006; Grethe and Moock, 1990). The cutoff of Tanimoto similarity coefficients was set as 0.70, and compounds above this value were chosen to assess drug-likeness rules by REOS rules (Walters et al., 1998) to remove

compounds with toxic, reactive, or otherwise undesirable moieties. From this, 21 compounds were chosen and purchased.

2.11. Virus production-infectivity assays

MT-4 cells were infected with HIV-1_{IIIB} at M.O.I of 0.03 in the presence of vehicle control or serial dilutions of TX-1918. After incubation at 37 °C for 2 h, cells were washed twice with PBS to remove free viruses and resuspended in RPMI-1640. Cells (10^6 in 500 µl) were next seeded in each well of a 24-well plate with the same concentration gradient as in the initial infections. After incubation for 3 days, supernatants were collected, and p24 levels were determined using a previously described in-house ELISA (Liu et al., 2007), and EC_{50} values were calculated.

Cells were collected, lysed for western blotting, and proteins were separated by SDS-PAGE and transferred to PVDF membranes. PVDF membranes were blocked with 5% milk for 1 h at room temperature and then incubated overnight with anti-HIV-1 p24 antibodies at 4 °C. Membranes were probed with HRP secondary antibodies at room temperature for 1 h. The membranes were washed thoroughly, stained with chemiluminescent HRP substrate, and exposed to X-ray film.

3. Results and discussion

3.1. Design of the assay

To identify novel compounds that interact with the CAI binding site in HIV-1 CA, we adopted an HTRF approach using biotinylated CAI peptide and GST-tagged CA CTD protein (Fig.1). Following CA CTD-CAI complex formation, fluorescent acceptor XL665-labeled streptavidin and donor europium cryptate conjugated anti-GST antibody HTRF reagents were added. Upon excitation at 340 nm, the donor fluorophore will be excited and emit at 615 nm, and if the acceptor fluorophore is in close proximity, there will be efficient energy transfer and the donor will emit at 665 nm. Accordingly, efficient energy transfer between the donor and acceptor will take place only upon CA CTD-CAI complex formation.

3.2. Optimization of HTRF-based CA CTD-CAI interaction assay

Recombinant CA CTD protein was purified from *E. coli* (> 95% purity as assessed by SDS-PAGE). Biolayer interferometry (BLI) is a label-free technology suitable for measuring biomolecular interactions (Renaud et al., 2016). We first performed a BLI assay to validate the interaction between GST-tagged CA CTD protein and CAI. As the binding events are monitored by the change in optical thickness of the sensor tip surface, it is recommended to immobilize the smaller binding partner to the tip and to keep the larger binding partner in solution to achieve a significant change of optical thickness upon analyte binding. We thus decided to use the same biotinylated CAI peptide that we also used for the HTRF assay for immobilization to the biosensor tips. CA CTD solutions were prepared in three different concentrations. After the sensorgrams were recorded, k_{on}, k_{dis} and K_D values were calculated by applying a global 1:1 fit to all curves. We obtained a K_D value of 7.0 nM (with $k_{on} = 2.1 \times 10^4$ $(M{\cdot}s)^{-1}$ and $k_{dis} = 1.52 \times 10^{-4}$ s^{-1}) for the binding of CA CTD to the immobilized biotin-CAI peptide (Fig. 2), revealing successful interaction of GST-CA CTD and the modified CAI peptide.

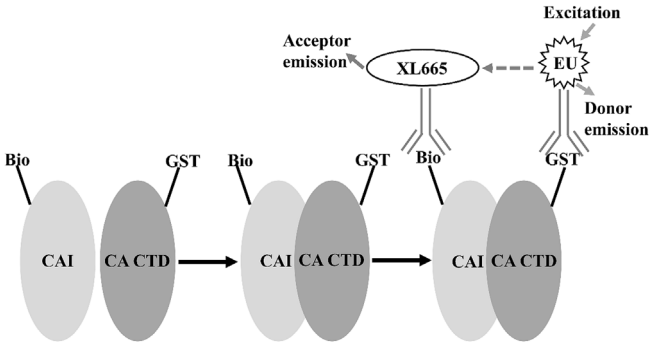

Fig. 1. Principle of the HTRF-based assay. The assay monitors the interaction between CAI-biotin peptide and glutathione-S-transferase (GST)-tagged CA CTD. The transfer of energy between two fluorophores, a donor and an acceptor labeled with europium cryptate (EU) and allophycocyanin (XL665) respectively, will yield HTRF signal upon protein-peptide interaction. Europium cryptate is excited at 320 nm, and emissions at 665 nm and 620 nm are measured. The HTRF signal is calculated from the 665 nm:620 nm emission ratio. The assay signal will drop in the presence of a molecule that competes with CAI for binding to CA CTD.

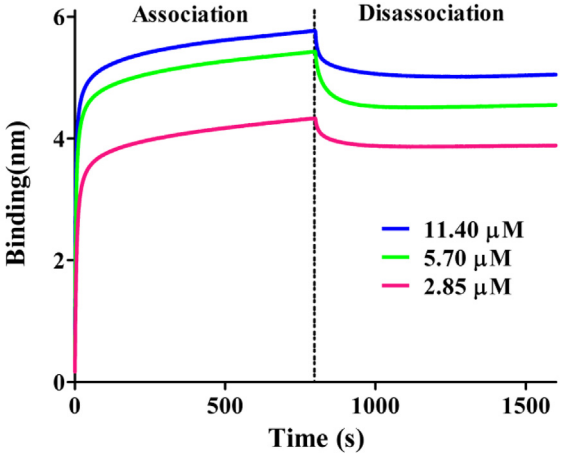

K_D (nM)	k_{on} (M·s)	k_{dis} (1/s)
7.00 ±0.17	$2.16 \pm 0.04 \times 10^4$	$1.52 \pm 0.03 \times 10^{-4}$

Fig. 2. Determination of K_D for CA CTD-CAI interaction. Association and dissociation sensorgrams were performed with various HIV-1 CA CTD concentrations using previously bio-CAI-loaded SA biosensors.

Development of robust high-throughput assays begins with the identification of an appropriate assay buffer. Previous buffer conditions in an AlphaScreen format for detecting CA CTD-CAI interactions allowed us to readily adapt buffer conditions for the current assay (Machara et al., 2016). Next, cross-titration experiments where both interacting partners were titrated against each other were performed to determine optimal concentrations of CA CTD and CAI for robust signal with as little protein as possible and to remain well below the hooking range. The hook effect occurs when the concentration of one of the interacting partners is increased beyond saturation of its antibody. Results from a representative cross-titration series are shown in Fig. 3A. The effect of hooking can clearly be seen at concentrations of 60 nM GST-CA CTD and higher. Under these conditions, the fluorescent donor GST antibody is expected to be fully saturated and excess CA CTD protein will compete with CA CTD on the donor surface for binding to CAI, effectively inhibiting the signal. With the concentration of CA CTD fixed at 30 nM, S/B ratios were calculated under different concentrations of CAI (Fig. 3B). Based on these results, we selected 30 nM CAI to achieve both high S/B and low peptide consumption rate.

Since protein-peptide interactions can be difficult to disrupt by small molecules, we aimed to screen at a relatively high compound concentration of 50 µM, which would impact the final concentration of dimethyl sulfoxide (DMSO) in the assay. To assess the tolerance of the assay for DMSO, we titrated it across the concentration range of 0.25%–10% (v/v). The HTRF signal was normalized to the 0% DMSO condition and corrected for background. Fig. 3C shows that despite a

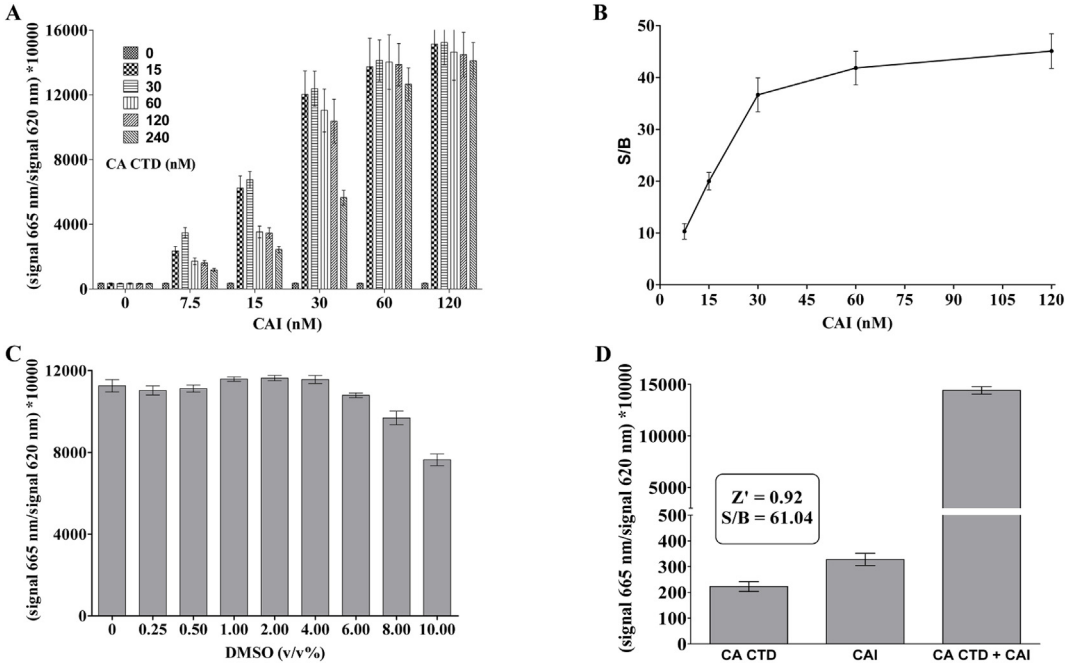

Fig. 3. Optimization of the HTRF-based competitive binding assay. **(A)** CA CTD and CAI were titrated against each other and the HTRF signal was measured. Results are average ± standard deviation for n = 3 independent experiments. **(B)** S/B ratios calculated under different concentration of CAI with CA CTD concentration fixed at 30 nM. The optimal condition contained 30 nM GST-CTD and 30 nM bio-CAI. **(C)** Tolerance for dimethylsulfoxide (DMSO) in the HTRF assay. DMSO was titrated down starting from 10% (v/v) in the CA CTD-CAI interaction assay. Results are average ± standard deviation for n = 3 independent experiments. **(D)** Statistics of the HTRF-based assay under the optimal conditions. Results are average ± standard deviation for n = 3 independent experiments.

high tolerance of the assay for DMSO, variability increased to unacceptable levels when more than 6% DMSO was present. Based on these results, the final DMSO concentration in the assay buffer was capped at 4%.

HTS assay optimization is a fine balance between identifying robust assay conditions with minimal variability and keeping costs acceptable. In the present case, costs were mainly driven by the amount of HTRF regents used. According to the manufacturer's instruction, XL665-conjugated streptavidin and MAb GST-Eu cryptate could be used at 0.75 nM and 3.63 nM respectively, while maintaining quality sufficiently robust for HTS. Thus, the final optimized assay mixture contained 30 nM bio-CAI, 30 nM GST-CA-CTD, 0.75 nM XL665-conjugated streptavidin and 3.63 nM Mab GST-Eu cryptate, under which the Z' and S/B values of the assay were respectively 0.92 and 61.04 (Fig. 3D).

3.3. Assay validation

The CAI peptide efficiently abrogates both immature and mature capsid assemblies in *vitro* as shown by electronic microscopy studies (Sticht et al., 2005). Therefore, untagged CAI was used to corroborate the ability of our assay to discover inhibitors. As depicted in Fig. 4A, assay signals were competed and inhibited by untagged CAI to background levels with an IC_{50} value of 6.5 μM (95% confidence interval [CI], 6.2 μM–6.8 μM), which was comparable to previous experiment result of 11.0 μM, validating that the assay can robustly detect decreases in signal and was therefore effective and suitable for drug screening applications (Machara et al., 2016).

To determine whether the assay was sufficiently sensitive to detect differences in compound binding affinity, we performed competition assays with various concentrations of taurocholic acid (TA), glycodeoxycholate (GDC), ebselen and trametinib. TA and GDC are CA-targeting inhibitors that interact with the same binding pocket as CAI, through at lower affinity than CAI (Lampel et al., 2015). In contrast, neither ebselen nor trametinib are expected to interact with the CAI binding pocket. Ebselen covalently binds the HIV-1 CA CTD via a selenylsulfide linkage with Cys 198 and Cys 218, neither of which locate at the interface of the CA CTD-CAI interaction (Thenin-Houssier et al., 2016). Trametinib is not known to target CA directly, instead abrogating the proper disassembly of the CA core by inhibiting ERK2 kinase phosphorylation levels inside virions (Dochi et al., 2018). At 50 μM concentration, unlabeled CAI reduced the signal to nearly background (Fig. 4A and B). In contrast, TA and GDC had comparatively weak inhibitory effects (less than 20%) at 50 μM, while at < 3.2%, ebselen and trametinib basically lacked inhibitory activity (Fig. 4B). These results confirm that the HTRF-based competition assay is capable of detecting differences in the relative binding affinity between compounds that interact with the CAI binding site on CA CTD.

To determine whether the assay can be miniaturized to 384-well plates for HTS, we performed a checkerboard assay. The assay yielded a Z' factor of 0.89 (Fig. 4C). Assays with a Z' of 0.5 or greater are considered excellent for HTS (Inglese et al., 2007). Therefore, the CAI competition assay has statistical properties that are desirable for HTS. The HTS protocol was outlined in Table 2.

3.4. Testing of the assay in HTS

To determine the utility of the assay in HTS, we performed a small-scale pilot screen of three protein kinase inhibitor libraries at a compound concentration of 50 μM. The set of test compounds consisted of 464 small molecules that were available at 10 mM concentrations in DMSO, thereby resulting in 0.5% (v/v) DMSO in the final assay mixture. Assay performance was evaluated on a plate-by-plate basis and remained robust throughout the entire screening campaign (Fig. 5A). A median Z′-factor of 0.78 was obtained and no plates failed during screening. Hits were scored as compounds that showed an inhibition ratio of the signal greater than 70%. The screen revealed one kinase inhibitor, TX-1918, that appeared to inhibit the interaction (Fig. 5B). This represented a 0.21% hit rate, which seemed appropriate for HTS (Zhu et al., 2013). The inhibitory effect of TX-1918 on the CA CTD-CAI interaction was confirmed by HTRF, which yielded an IC_{50} of 3.81 μM

A

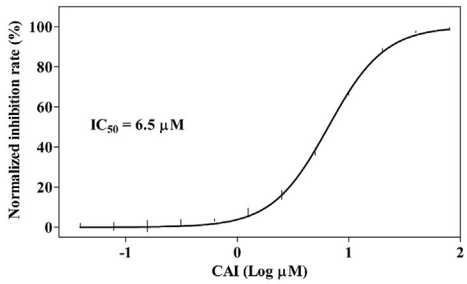

C

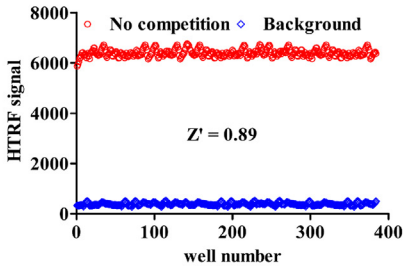

B

Compounds	Inhibitory rate at 50 μM (%)	Structure/sequence
CAI	99.42 ± 0.25	ITFEDLLDYYG
TA	17.88 ± 0.71	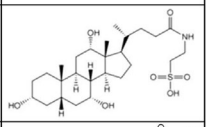
GDC	10.52 ± 0.38	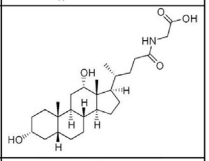
Ebselen	3.14 ± 0.13	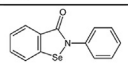
Trametinib	2.75 ± 0.46	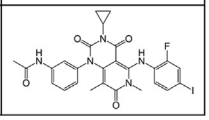

Fig. 4. Validation of the assay with competitor CAI and determination of Z' factor. **(A)** Test of the response of the assay to unlabeled CAI at various concentrations in 96-well plates. **(B)** Comparison of inhibitory effect of different compounds on the CA CTD-CAI interaction. Panel A and B results are averages ± standard deviation for n = 3 independent experiments. **(C)** Results of the checkerboard evaluation of the assay in 384-well plates.

(Fig. 5C).

We have developed a biochemical target-based assay based on the competition of binding of peptide CAI to the HIV-1 CA CTD. The assay has properties desirable for HTS, including a simple mix-and-read endpoint format, a stable endpoint, relatively low reagent cost, and excellent statistical properties.

False positives often dominate initial hit lists obtained from HTS campaigns. In this HTRF-based assay, false-positives may interfere by competing with CAI-bio for streptavidin, or by competing with CA-CTD for anti-GST antibody binding. This limitation may be overcome by a counter-screen using biotinylated GST-tag protein after the primary screen. Additionally, several biophysical approaches for direct binding analysis, such as surface plasmon resonance (SPR) and BLI, may be used as orthogonal assays to validate hits.

3.5. TX-1918 inhibits HIV-1-induced syncytia formation

TX-1918 was identified using our HTS-HTRF screen for inhibitors of the CA CTD-CAI interaction. To further evaluate the antiviral effects of TX-1918, we tested the compound for protecting C8166 cells from HIV-1-induced cytopathic effects (CPE). The cytotoxic effect of TX-1918 on C8166 cells was also assessed. As shown in Fig. 6A, TX-1918 moderately inhibited HIV-1_{IIIB} induced CPE, with an EC_{50} value of 15.16 μM. However, TX-1918 revealed limited therapeutic value because its half maximal cytotoxic concentration (CC_{50}) was 20.80 μM, yielding a SI value of 1.34. Although TX-1918 could not be used as an antiviral drug, it could serve as a lead compound to discover pharmacologically-relevant compounds. We accordingly used TX-1918 to search the ChemDiv database based on similarity, which yielded a total of 21 novel compounds. K815-0041, which was one of the more potent compounds identified, displayed EC_{50} and CC_{50} values of 6.57 μM and 102.55 μM respectively, yielding a SI of 15.60 (Fig. 6A). The structures of the 20 additional compounds from the similarity search together with their CC_{50} and EC_{50} values can be found in Fig. S1.

3.6. Virus production-infectivity assays

To assess antiviral activity under conditions more quantitative than manually counting syncytia formation, supernatants of infected MT-4 T cell cultures treated with various concentrations of TX-1918 were analyzed by p24 ELISA. As shown in Fig. 6B, TX-1918 inhibited the production of infectious virus with an EC_{50} of 3.60 μM, which was improved from the EC_{50} value determined by the CPE assay (Fig. 6A). Thus, the SI of TX-1918 in MT-4 cells was 6.6 (Fig. 6B). The infected cell cultures were analyzed by anti-p24 immunoblotting to assess potential inhibitory effects on CA p24 production and/or Gag Pr55 functionality. These data revealed significant reductions in proteolyzed CA p24 with increasing concentrations of TX-1918, suggesting that TX-1918 inhibited Gag polyprotein processing (Fig. 6B).

Table 2
HTS protocol table.

Step	Parameter	Value	Description
1	Controls	1 μl	DMSO (negative), buffer (positive) and untagged CAI (positive compound)
2	Library compounds	1 μl	50 μM, duplicate
3	Proteins	2 μl for each	Bio-CAI (30 nM), CA-CTD (30 nM)
4	Incubation time	30 min	Ambient temperature
5	Regents	2.5 μl for each	Anti-GST europium cryptate (3.63 nM) and XL665-conjungated streptavidin (0.75 nM)
6	Incubation time	1 h	Ambient temperature
7	Assay readout	665 nm and 620 nm	Envision multilabel reader, TR-FRET mode

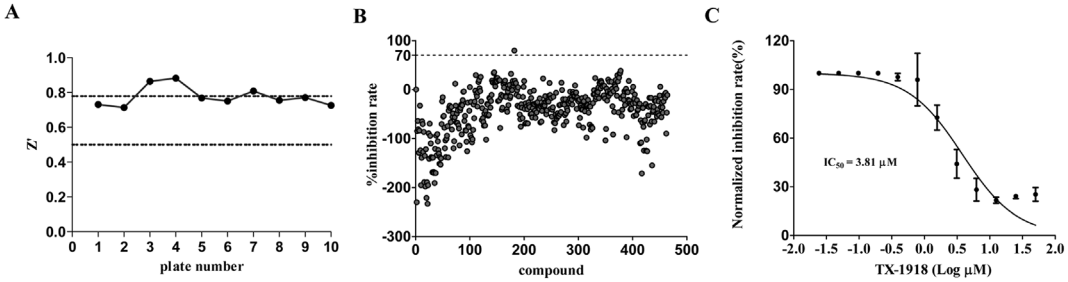

Fig. 5. Protein kinase inhibitor library screens. **(A)** Assay performance throughout the screening campaign. The median Z′-factor of 0.78 was determined across the indicated per plate samples. **(B)** Results of the screening of the three libraries (464 compounds). The gray dashed line indicates cut-off of 70% inhibition. The single hit above this line is TX-1918. **(C)** Inhibition of the CA CTD-CAI interaction by TX-1918 in the HTRF assay. Results are average ± standard deviation for n = 3 independent experiments.

3.7. Effects of TX-1918 on CA assembly in vitro

To determine the effects of TX-1918 on CA assembly in an isolated system, *in vitro* assembly assays were performed using WT CA protein purified following its expression in *E. coli*. WT CA protein incubated in the presence of high salt spontaneously assembles into higher-order forms including nanotubes, which can be monitored by absorbance at 350 nm. The CAI peptide, which was used as a positive control, inhibited in a dose dependent manner both the rate and extent of CA assembly (Fig. 7A). TX-1918 similarly in a dose dependent manner inhibited both the rate and extent of CA assembly, though was clearly less potent than CAI at the highest concentration tested (Fig. 7B). Our results demonstrate that TX-1918 inhibits the interaction of CAI with CA CTD (Fig. 5C), interfers with Pr55 Gag proteolysis (Fig. 6B), and inhibits CA assembly *in vitro* (Fig. 7).

In conclusion, the HTRF-based assay that we developed should be useful to screen large compound libraries to identify novel chemical scaffolds that interact with the specific binding site of CAI on the HIV-1 CA CTD, thus expanding the chemical space for the development of CA-targeting antiviral drugs.

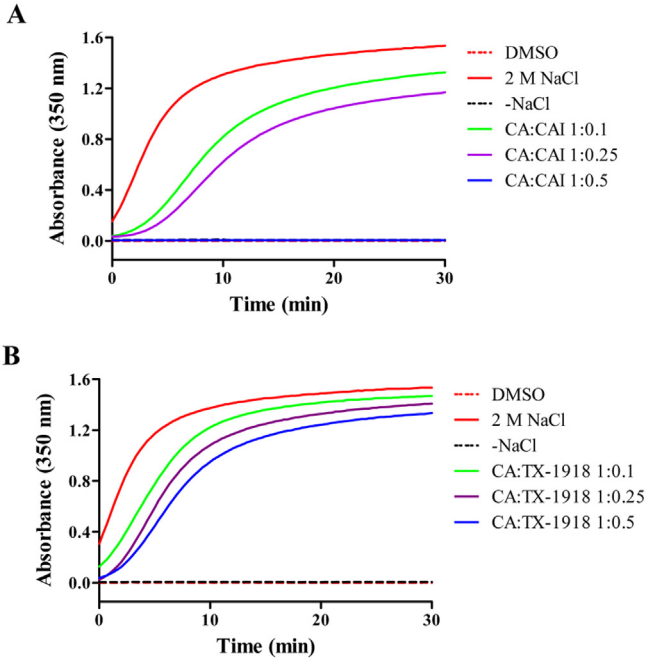

Fig. 7. Impact of TX-1918 on NaCl-dependent *in vitro* CA assembly. **(A)** Effect of CAI on *in vitro* CA assembly. **(B)** Effect of TX-1918 on *in vitro* CA assembly. Results are representative of those obtained in 2 independent experiments.

Declaration of conflicting interests

The author(s) declared no potential conflicts of interest with respect to the research, authorship, and/or publication of this article.

Funding

This work was supported by the National Natural Science Foundation of China (Nos. 31700297, 81603152 and 81102483),

A

Compound	CC_{50} (μM)	EC_{50} (μM)	SI	Structure
TDF	> 100	0.0084 ± 0.0015	> 11904.76	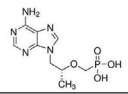
TX-1918	20.80±3.21	15.16 ± 5.34	1.34	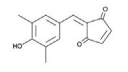
K815-0041	102.55±25.29	6.57 ± 2.60	15.60	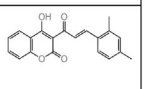

B

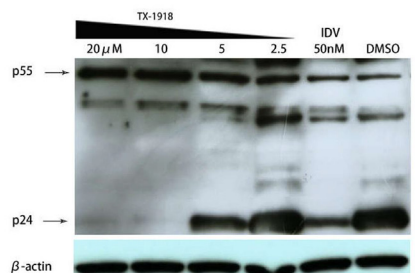

CC_{50}	MTT	23.65 ± 1.12 μM
EC_{50}	p24	3.60 ± 0.54 μM

Fig. 6. Activity of compounds against HIV-1 replication. **(A)** Antiviral effects of TX-1918 and K815-0041 determined in the CPE assay after infection of C8166 cells. CC_{50} values on C8166 cells as well as SI values are shown. TDF served as positive control. **(B)** Effect of TX-1918 on multiple rounds of HIV-1_{IIIB} replication. MT-4 cell lysates following 3 days of HIV-1 replication in the presence of the indicated concentration of TX-1918 or vehicle control (DMSO) were probed with anti-CA antibodies. The protease inhibitor IDV was used as a positive control. Associated EC_{50} value for inhibition of p24 via ELISA and MT-4 cell CC_{50} value are shown. Results are average ± standard deviation for n = 3 independent experiments. The gel image is representative of results obtained in 2 independent experiments.

Innovation and Entrepreneurship Program 2017 of Jiangsu Province, Jiangsu Overseas Visiting Scholar Program for University Prominent Young & Middle-aged Teachers and Presidents, Natural Science Foundation of Jiangsu Province (BK20170311 and BK20170312). Industry-Academia Cooperation Innovation Fund Project of Jiangsu Province (BY201603006 and BY201603011), Six Talent Peaks Project in Jiangsu Province (2016XYDXXJS020), the Special Program for Applied Research on Super Computation of the NSFC Guangdong Joint Fund (U1501501), the Fund from Jiangsu Education Department (16KJD310001) and the United States National Institutes of Health (P50 GM082251 and T32 AI007386). The authors thank national compound resource center (Shanghai, China) for supplying the small compounds used in this study.

Appendix A. Supplementary data

Supplementary data to this article can be found online at https://doi.org/10.1016/j.antiviral.2019.104544.

References

Ali, S.A., Teow, S.Y., Omar, T.C., Khoo, A.S.B., Choon, T.S., Yusoff, N.M., 2016. A cell internalizing antibody targeting capsid protein (p24) inhibits the replication of HIV-1 in T cells lines and PBMCs: a proof of concept study. PLoS One 11, e0145986. https://doi.org/10.1371/journal.pone.0145986.

Blair, W.S., Pickford, C., Irving, S.L., Brown, D.G., Anderson, M., Bazin, R., Hunt, R., 2010. HIV capsid is a tractable target for small molecule therapeutic intervention. PLoS Pathog. 6, e1001220. https://doi.org/10.1371/journal.ppat. 1001220.

Campbell, E.M., Hope, T.J., 2015. HIV-1 capsid: the multifaceted key player in HIV-1 infection. Nat. Rev. Microbiol. 13, 471–483. https://doi.org/10.1038/nrmicro 3503.

Carnes, S.K., Sheehan, J.H., Aiken, C., 2018. Inhibitors of the HIV-1 capsid, a target of opportunity. Curr. Opin. HIV AIDS 13, 359–365. https://doi.org/10.1097/COH. 0000000000000472.

Chaudhuri, S., Symons, J.A., Deval, J., 2018. Innovation and trends in the development and approval of antiviral medicines: 1987-2017 and beyond. Antivir. Res. 155, 76–88. https://doi.org/10.1016/j.antiviral.2018.05. 005.

Chen, N.Y., Zhou, L., Gane, P.J., Opp, S., Ball, N.J., Nicastro, G., Diaz-Griffero, F., 2016. HIV-1 capsid is involved in post-nuclear entry steps. Retrovirology 13, 28. https://doi.org/10.1186/s12977-016-0262-0.

Curreli, F., Zhang, H., Zhang, X., Pyatkin, I., Victor, Z., Altieri, A., Debnath, A.K., 2011. Virtual screening based identification of novel small-molecule inhibitors targeted to the HIV-1 capsid. Bioorg. Med. Chem. 19, 77–90. https://doi.org/10.1016/j.bmc. 2010.11.045.

Dochi, T., Akita, A., Kishimoto, N., Takamune, N., Misumi, S., 2018. Trametinib suppresses HIV-1 replication by interfering with the disassembly of human immunodeficiency virus type 1 capsid core. Biochem. Biophys. Res. Commun. 495, 1846–1850. https://doi.org/10.1016/j.bbrc.2017.11.177.

Elena, S.F., 2012. RNA virus genetic robustness: possible causes and some consequences. Curr. Opin. Virol. 2, 525–530. https://doi.org/10.1016/j.coviro. 2012.06.008.

Engelman, A., Cherepanov, P., 2012. The structural biology of HIV-1: mechanistic and therapeutic insights. Nat. Rev. Microbiol. 10, 279–290. https://doi.org/10.1038/nrmicro2747.

Grethe, G., Moock, T.E., 1990. Similarity searching in REACCS. A new tool for the synthetic chemist. J. Chem. Inf. Comput. Sci. 30, 511–520. https://doi.org/10.1021/ci00068a025.

Hel, Z., McGhee, J.R., Mestecky, J., 2006. HIV infection: first battle decides the war. Trends Immunol. 27, 274–281. https://doi.org/10.1016/j.it.2006.04.007.

Inglese, J., Johnson, R.L., Simeonov, A., Xia, M., Zheng, W., Austin, C.P., Auld, D.S., 2007. High-throughput screening assays for the identification of chemical probes. Nat. Chem. Biol. 3, 466–479. https://doi.org/10.1038/nchembio.2007. 17.

Kortagere, S., Madani, N., Mankowski, M.K., Schön, A., Zentner, I., Swaminathan, G., Passic, S.R., 2012. Inhibiting early-stage events in HIV-1 replication by small-molecule targeting of the HIV-1 capsid. J. Virol. 86, 8472–8481. https://doi.org/10.1128/JVI.05006-11.

Kortagere, S., Xu, J.P., Mankowski, M.K., Ptak, R.G., Cocklin, S., 2014. Structure activity relationships of a novel capsid targeted inhibitor of HIV-1 replication. J. Chem. Inf. Model. 54, 3080–3090. https://doi.org/10.1021/ci500437r.

Kožíšek, M., Štěpánek, O., Parkan, K., Albiñana, C.B., Pávová, M., Weber, J., Machara, A., 2016. Synthesis and evaluation of 2-pyridinylpyrimidines as inhibitors of HIV-1 structural protein assembly. Bioorg. Med. Chem. Lett 26, 3487–3490. https://doi.org/10.1016/j.bmcl.2016.06.039.

Lampel, A., Bram, Y., Ezer, A., Shaltiel-Kario, R., Saad, J., Bacharach, E., Gazit, E., 2015. Targeting the early step of building block organization in viral capsid assembly. ACS Chem. Biol. 10, 1785–1790. https://doi.org/10.1021/acsch embio. 5b00347.

Lamorte, L., Titolo, S., Lemke, C.T., Goudreau, N., Mercier, J.F., Wardrop, E., Aiken, C., 2013. Discovery of novel small-molecule HIV-1 replication inhibitors that stabilize capsid complexes. Antimicrob. Agents Chemother. 57, 4622–4631. https://doi.org/10.1021/acschembio.5b00347.

Lanman, J., Sexton, J., Sakalian, M., Prevelige Jr., P.E., 2002. Kinetic analysis of the role of intersubunit interactions in human immunodeficiency virus type 1 capsid protein assembly *in vitro*. J. Virol. 76, 6900–6908. https://doi.org/10.1128/JVI.76.14.6900-6908.2002.

Lemke, C.T., Titolo, S., von Schwedler, U., Goudreau, N., Mercier, J.F., Wardrop, E., Gagnon, A., 2012. Distinct effects of two HIV-1 capsid assembly inhibitor families that bind the same site within the N-terminal domain of the viral CA protein. J. Virol. 86, 6643–6655. https://doi.org/10.1128/JVI.00493-12.

Lemke, C.T., Goudreau, N., Faucher, A.M., Mason, S.W., Bonneau, P., 2013. A novel inhibitor-binding site on the HIV-1 capsid N-terminal domain leads to improved crystallization via compound-mediated dimerization. Acta Crystallogr. D: Biol. Crystallogr. 69, 1115–1123. https://doi.org/10.1107/S0907444913006409.

Liu, G.J., Wang, J.P., Xiao, J.C., Zhao, Z.W., Zheng, Y.T., 2007. Preparation and characterization of three monoclonal antibodies against HIV-1 p24 capsid protein. Cell. Mol. Immunol. 4, 203–208.

Machara, A., Lux, V., Kožíšek, M., Grantz Šašková, K., Štěpánek, O., Kotora, M., Parkan, K., Pávová, M., Glass, B., Sehr, P., Lewis, J., Müller, B., Kräusslich, H., Konvalinka, J., 2016. Specific inhibitors of HIV capsid assembly binding to the C-Terminal domain of the capsid protein: evaluation of 2-arylquinazolines as potential antiviral compounds. J. Med. Chem. 59, 545–558. https://doi.org/10.1021/acs.jmedchem.5b01089.

Perrier, M., Bertine, M., Le Hingrat, Q., Joly, V., Visseaux, B., Collin, G., Charpentier, C., 2017. Prevalence of gag mutations associated with in vitro resistance to capsid inhibitor GS-CA1 in HIV-1 antiretroviral-naive patients. J. Antimicrob. Chemother. 72, 2954–2955. https://doi.org/10.1093/jac/dkx208.

Price, A.J., Jacques, D.A., McEwan, W.A., Fletcher, A.J., Essig, S., Chin, J.W., James, L.C., 2014. Host cofactors and pharmacologic ligands share an essential interface in HIV-1 capsid that is lost upon disassembly. PLoS Pathog. 10, e1004459. https://doi.org/10.1371/journal.ppat.1004459.

Rihn, S.J., Wilson, S.J., Loman, N.J., Alim, M., Bakker, S.E., Bhella, D., Bieniasz, P.D., 2013. Extreme genetic fragility of the HIV-1 capsid. PLoS Pathog. 9, e1003461. https://doi.org/10.1371/journal.ppat.1003461.

Renaud, J.P., Chung, C.W., Danielson, U.H., Egner, U., Hennig, M., Hubbard, R.E., Nar, H., 2016. Biophysics in drug discovery: impact, challenges and opportunities. Nat. Rev. Drug Discov. 15, 679–698. https://doi.org/10.1038/nrd.2016.123.

Shi, J., Zhou, J., Shah, V.B., Aiken, C., Whitby, K., 2011. Small-molecule inhibition of human immunodeficiency virus type 1 infection by virus capsid destabilization. J. Virol. 85, 542–549. https://doi.org/10.1128/JVI.01406-10.

Sticht, J., Humbert, M., Findlow, S., Bodem, J., Müller, B., Dietrich, U., Werner, J., Kräusslich, H., 2005. A peptide inhibitor of HIV-1 assembly in vitro. Nat. Struct. Mol. Biol. 12, 671–677. https://doi.org/10.1038/nsmb964.

Tang, C., Loeliger, E., Kinde, I., Kyere, S., Mayo, K., Barklis, E., Summers, M.F., 2003. Antiviral inhibition of the HIV-1 capsid protein. J. Mol. Biol. 327, 1013–1020. https://doi.org/10.1016/S0022-2836(03)00289-4.

Tedbury, P.R., Freed, E.O., 2015. HIV-1 gag: an emerging target for antiretroviral therapy. In: The Future of HIV-1 Therapeutics. Springer International Publishing, pp. 171–201. https://doi.org/10.1007/82_2015_436.

Ternois, F., Sticht, J., Duquerroy, S., Kräusslich, H.G., Rey, F.A., 2005. The HIV-1 capsid protein C-terminal domain in complex with a virus assembly inhibitor. Nat. Struct. Mol. Biol. 12, 678–682. https://doi.org/10.1038/nsmb967.

Thenin-Houssier, S., De Vera, I.M.S., Pedro-Rosa, L., Brady, A., Richard, A., Konnick, B., Billack, B., 2016. Ebselen, a small-Molecule capsid inhibitor of HIV-1 replication. Antimicrob. Agents Chemother. 60, 2195–2208. https://doi.org/10.1128/AAC.02574-15.

Tse, W.C., Link, J.O., Mulato, M., 2017. Discovery of novel potent HIV capsid inhibitors with long-acting potential. Abstract No. 38. In: 24th Conference on Retroviruses and Opportunistic Infections.

Urano, E., Kuramochi, N., Ichikawa, R., Murayama, S.Y., Miyauchi, K., Tomoda, H., Morikawa, Y., 2011. Novel postentry inhibitor of human immunodeficiency virus type 1 replication screened by yeast membrane-associated two-hybrid system. Antimicrob. Agents Chemother. 55, 4251–4260. https://doi.org/10.1128/AAC.00299-11.

Vozzolo, L., Loh, B., Gane, P.J., Tribak, M., Zhou, L., Anderson, I., Fassati, A., 2010. Gyrase B inhibitor impairs HIV-1 replication by targeting Hsp90 and the capsid protein. J. Biol. Chem. 285, 39314–39328. https://doi.org/10.1074/jbc.M110.155275.

Walters, W.P., Stahl, M.T., Murcko, M.A., 1998. Virtual screening-an overview. Drug Discov. Today 3, 160–178. https://doi.org/10.1016/S1359-6446(97)01163-X.

Wang, J.H., Tam, S.C., Huang, H., Ouyang, D.Y., Wang, Y.Y., Zheng, Y.T., 2004. Site-directed PEGylation of trichosanthin retained its anti-HIV activity with reduced potency *in vitro*. Biochem. Biophys. Res. Commun. 317, 965–971. https://doi.org/10.1016/j.bbrc.2004.03.139.

Wang, R.R., Gao, Y.D., Ma, C.H., Zhang, X.J., Huang, C.G., Huang, J.F., Zheng, Y.T., 2011. Mangiferin, an anti-HIV agent targeting protease effective against resistant strains. Molecules 16, 4264–4277. https://doi.org/10.3390/molecules 16054264.

Willett, P., 2006. Similarity-based virtual screening using 2D fingerprints. Drug Discov. Today 11, 1046–1053. https://doi.org/10.1016/j.drudis.2006.10.005.

Zhang, X., 2018. Anti-retroviral drugs: current state and development in the next decade. Acta Pharm. Sin. B. 8, 131–136. https://doi.org/10.1016/j.apsb.2018. 01.012.

Zhang, H., Zhao, Q., Bhattacharya, S., Waheed, A.A., Tong, X., Hong, A., Freed, E.O., 2008. A cell-penetrating helical peptide as a potential HIV-1 inhibitor. J. Mol. Biol. 378, 565–580. https://doi.org/10.1016/j.jmb.2008.02.066.

Zhang, J.H., Chung, T.D., Oldenburg, K.R., 1999. A simple statistical parameter for use in evaluation and validation of high throughput screening assays. J. Biomol. Screen 4, 67–73. https://doi.org/10.1177/108705719900400206.

Zhang, H., Curreli, F., Zhang, X., Bhattacharya, S., Waheed, A.A., Cooper, A., Debnath, A.K., 2011. Antiviral activity of α-helical stapled peptides designed from the HIV-1 capsid dimerization domain. Retrovirology 8, 28. https://doi.org/10.1186/1742-

4690-8-28.
Zhang, H., Curreli, F., Waheed, A.A., Mercredi, P.Y., Mehta, M., Bhargava, P., Summers, M.F., 2013. Dual-acting stapled peptides target both HIV-1 entry and assembly. Retrovirology 10, 136. https://doi.org/10.1186/1742-4690-10-136.

Zhu, T., Cao, S., Su, P.C., Patel, R., Shah, D., Chokshi, H.B., Hevener, K.E., 2013. Hit identification and optimization in virtual screening: practical recommendations based on a critical literature analysis: miniperspective. J. Med. Chem. 56, 6560–6572. https://doi.org/10.1021/jm301916b.